Electronic Supplementary Material (ESI) for Sustainable Energy & Fuels.

High Capacity Graphite-like Calcium Boridecarbide as a Novel Anode Active Material for Lithium-ion Batteries.

Go Tei*, Ryohei Miyamae, and Akira Kano

Technology Innovation Division, Panasonic Corporation, 1006 Oazakadoma, Kadoma-shi, Osaka 571-8501, Japan

E-mail: tei.go@jp.panasonic.com

Experimental Section

Material synthesis and Characterization

For synthesis of $Ca_{0.6}B_{1.2}C_{4.8}$, graphite powders (ca. 20 μm, Kojundo Chemical Lab. Co., Ltd.), CaB_6 (Sigma-Aldrich Co. LLC), and CaC_2 (FUJIFILM Wako Pure Chemical Industries Corp.) were mixed in an agate mortar at a stoichiometric ratio. All processes for preparing the mixture were carried out in an argon glove box where the O_2 and H_2O levels were kept below 5 ppm. Then, the mixture was heat treated in a graphite furnace under Ar flow at 2073 K for 5 hours. $Ca_{0.75}B_{1.5}C_{4.5}$ was synthesized in the same way, although the heat treatment temperature was 1773 K as in a previous report [1].

The X-ray diffraction (XRD) measurement was performed by MiniFlex 600 (Rigaku Corp., Japan) with Cu-Kα radiation. Rietveld refinement of synthesized $Ca_{0.6}B_{1.2}C_{4.8}$ was carried out using the RIETAN-FP program [2] (Fig. S1). The lattice parameters were initially set to those of $Ca_{0.75}B_{1.5}C_{4.5}$, which belongs to the space group of P6/mmm with hexagonal symmetry. The scale factor, zero point, background, lattice parameters, and occupancy parameter of the calcium atom were sequentially refined. The displacement parameters were set to 0.5. The fitted lattice parameters and R values are summarized in Table 1. XRD patterns of synthesized $Ca_{0.75}B_{1.5}C_{4.5}$ and $Ca_{0.6}B_{1.2}C_{4.8}$ are compared in Fig. S2. The (101), (110) and (103) peak positions of $Ca_{0.6}B_{1.2}C_{4.8}$ shift to lower diffraction angles compared with $Ca_{0.75}B_{1.5}C_{4.5}$ through (001) or (002) peak positions located at almost identical positions. This indicates that $Ca_{0.6}B_{1.2}C_{4.8}$ has a shorter side length of the hexagonal boron or carbon six-ring-forming boron-doped graphene layer than that of $Ca_{0.75}B_{1.5}C_{4.5}$, although there is no significant difference in interlayer distance. XRD patterns during the discharge/charge process (Fig. 3a) were observed using the extracted cathode electrode from laminate test cells, whose discharge/charge tests were stopped at corresponding observation points.

Table S2 depicts the atomic concentration ratio of carbon, boron and calcium atoms in the synthesized $Ca_{0.6}B_{1.2}C_{4.8}$ and $Ca_{0.75}B_{1.5}C_{4.5}$ by inductively coupled plasma atomic emission spectroscopy (ICP). In ICP measurement, CIROS-120 (SPECTRO Analytical Instruments GmbH) was used. First, the sample's weight was measured in a dry glove box where the H_2O level was kept below 10 ppm. Then, the sample was calcinated at 1073 K for 2 hours under atmospheric conditions, and the residue was alkali fusion-treated by sodium hydroxide and sodium peroxide. Finally, the melt was dissolved in hydrochloric acid and diluted by purified water for the measurement. The contents of boron and calcium in the sample were determined by ICP, and the remaining part of the mass was attributed to carbon.

X-ray photoelectron spectroscopy (XPS) was performed by PHI 5000

Versaprobe (ULVAC-PHI, Inc., Japan) with monochrome Al-Ka radiation. To prevent exposure of samples to the atmosphere, a sealed jig was used for moving samples from the argon glove box to the measuring chamber. Peak separation was performed by the XPSPEAK program [3].

Electrochemistry

Electrode preparation and cell assembly were carried out in a dry glovebox where the H_2O level was kept below 10 ppm. A slurry for preparing cathode electrodes was prepared by mixing active materials with acetylene black (AB, Denka Company Ltd.) as conductive additives and polyvinylidene fluoride (PVdF, Kureha Corp.) or polyimide (PI, I.S.T. Corp.) as a binder in N-methyl-2-pyrrolidone solvent (NMP, KISHIDA CHEMICAL Co., Ltd., battery grade). The weight ratio of active material, AB, and PVdF was set to 7:2:1. The slurry was coated on Cu foil and dried in a vacuum drying oven at 120℃. Before assembling a laminate-type cell, the laminates and separators were dried at 120℃. Lithium metal was used as a negative electrode. The electrolyte was 1M $LiPF_6$ in ethylene carbonate (EC)–ethyl methyl carbonate (EMC) electrolyte (KISHIDA CHEMICAL Co., Ltd., battery grade).

All charge/discharge tests were performed by a battery charge/discharge system (TOSCAT-3100, TOYO SYSTEM CO., LTD.) at room temperature. The rate was set to 3.72 mA/g and cut-off potential was set to 0 and 3 V vs. Li/Li^+. All tests were started from discharge (intercalation of lithium to active material). For extracting calcium atoms as pretreatment before obtaining the results in Fig. 4a, a positive constant current with a rate of 3.72 mA/g was applied allowing potential sweeping over 3 V vs. Li/Li^+ (Fig. S3).

First principle calculation

Density functional theory (DFT) calculations were used for estimating the change in interlayer distance of $Ca_{0.6}B_{1.2}C_{4.8}$ by lithium intercalation (Fig. 3b). The assumed structures are shown in Fig. S4. The VASP code [5, 6] was used with the Perdew-Burke-Ernzerhof (PBE) functional [7, 8], and the van der Waals interaction was determined by the DFT-D3 method with Becke-Jonson damping [9, 10]. Supercells containing 10 formula units of $Ca_{0.6}B_{1.2}C_{4.8}$ or $LiCa_{0.6}B_{1.2}C_{4.8}$ were set for the calculations (Fig. 3b). The k-point sampling was performed with a 6 × 6 × 3 mesh, and the plane-wave cutoff was set to 600 eV. Geometric relaxations were performed until the forces acting on ions were less than 0.005 eV $Å^{-1}$ per atom.

Discussion about the difference in configurations of Ca and Li atoms in interlayer

Comparing $Ca_{0.6}B_{1.2}C_{4.8}$ to $Ca_{0.75}B_{1.5}C_{4.5}$, 0.15 Ca atoms decreased per 6 B or C atoms whereas 0.38 Li atoms increased for capable of being intercalated per 6 B or C atoms (from 0.88 Li for $Ca_{0.75}B_{1.5}C_{4.5}$ to 1.26 Li for $Ca_{0.6}B_{1.2}C_{4.8}$). The difference in these two values can be explained by the difference of occupying area of Ca and Li atoms on the plane parallel to boron-doped graphene layers. In $Ca_{0.6}B_{1.2}C_{4.8}$ and $Ca_{0.75}B_{1.5}C_{4.5}$, the B-C bonding in an sp2 configuration contains π-bonding orbital occupied by a C $2p_z$ electron and a Ca 4s electron transferred to the B $2p_z$ orbital [1, 11]. After donating two 4s electrons to B $2p_z$ orbitals, Ca atoms become divalent cation states, which are highly repulsive with other cation atoms on the planes parallel to boron-doped graphene layer. On the other hand, lithium atoms, which form monovalent cation states and less ionized in the absence of interacting with already occupied B $2p_z$ orbitals by electrons from Ca atoms, should be less repulsive with other cations and occupy smaller areas than Ca atoms. As the result, removing one Ca atom can cause increase of more than one Li atoms capable of being intercalated. For verifying this hypothesis, we performed a DFT calculation to elucidate the difference in configuration of Ca and Li atoms in the interlayer. First, a realization of configuration of 10 formula unit of $Ca_{0.6}B_{1.2}C_{4.8}$ was prepared (Fig. S5 a). Ca atoms were set to uniformly distribute in the interlayer accompanied by two boron atoms at the nearest lattice points in the boron doped graphene layers. This configuration is assumed because the interaction between Ca atoms and B atoms in the born-doped graphene layers as explained above. Then, we added Li atoms to the structure to set the composition to be 10 formula unit of $LiCa_{0.6}B_{1.2}C_{4.8}$ (Fig. S5 b). Li atoms were uniformly distributed and located at the centers of hexagons formed by the lattice points. The configurations before and after structure relaxation were shown in Fig. S5 c. Compared with the initial structure, Ca atoms do not change their positions by structure relaxation. It is because Ca atoms are trapped by B atoms by ion interaction. On the other hand, Li atoms change their positions moving away from Ca atoms as indicated using the arrows in Fig. S5 c. As the result, Li atoms form some dense regions accommodating three Li atoms away from the regions occupied by Ca atoms as indicated by green circles in Fig.S5 c. The area of these dense regions is comparable with that of one pre-existing Ca atom occupies. If one Ca atom is removed, one such dense regions of Li atoms can be accommodated in interlayer. This is the reason that removing one Ca atom can cause increase of more than one Li atoms capable of being intercalated.

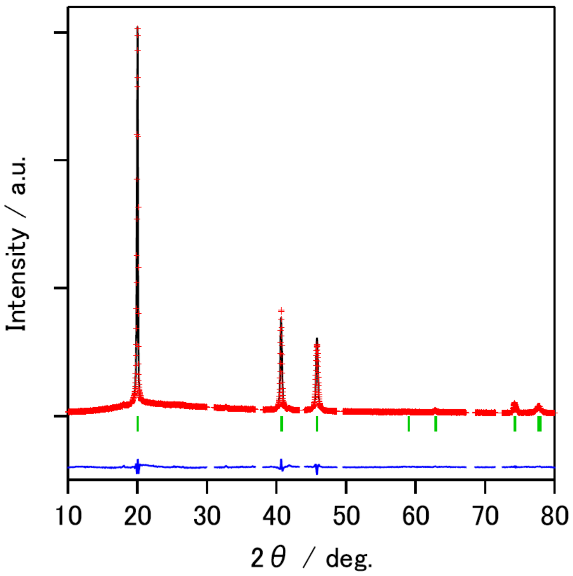

Fig. S1 Measured (red cross) and fitted (black line) patterns of synthesized $Ca_{0.6}B_{1.2}C_{4.8}$ and their difference (blue line). Green marks indicate the reflection positions of the $Ca_{0.6}B_{1.2}C_{4.8}$ with the fitted parameters. Regions corresponding to reflection positions of CaB6 were omitted in refinement. $R_{wp} = 0.06058$, $R_p = 0.04680$, $R_B = 0.03541$, $R(F^2) = 0.03095$, $\chi^2 = 1.237$.

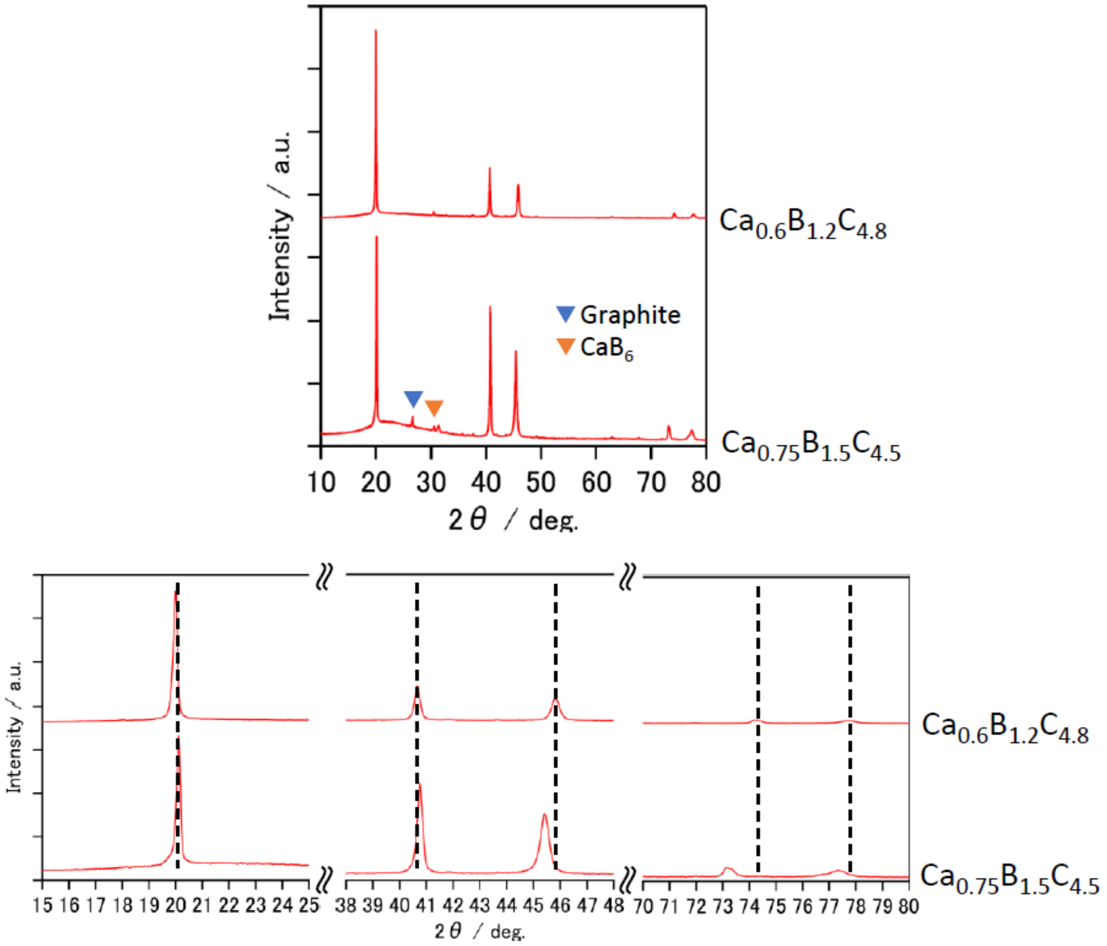

Fig. S2 Comparison of XRD patterns of synthesized $Ca_{0.6}B_{1.2}C_{4.8}$ and $Ca_{0.75}B_{1.5}C_{4.5}$.

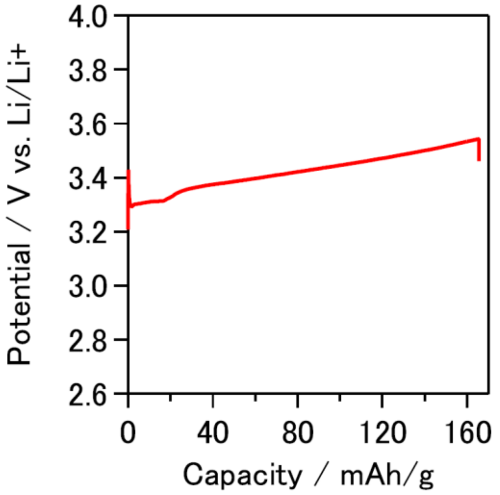

Fig. S3 Potential profile for calcium extraction from $Ca_{0.6}B_{1.2}C_{4.8}$ electrode by applying positive constant current.

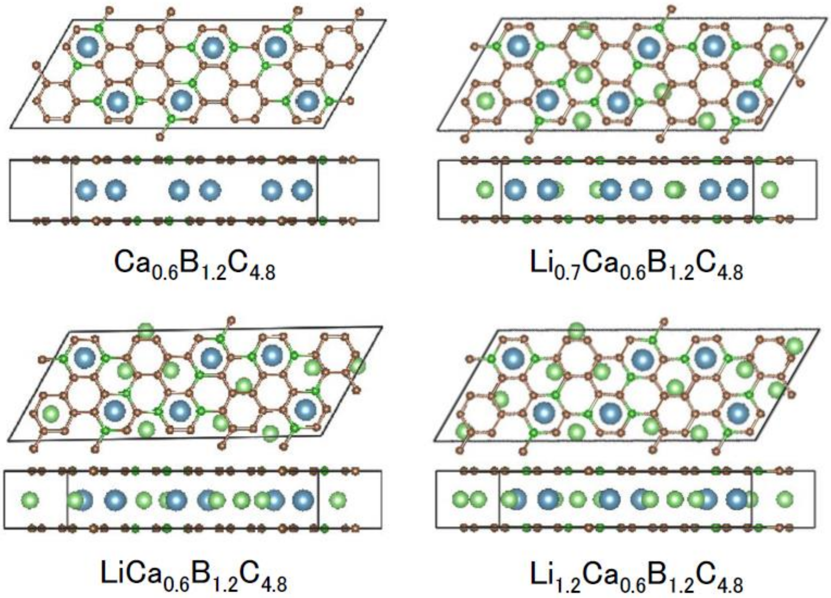

$Ca_{0.6}B_{1.2}C_{4.8}$

$Li_{0.7}Ca_{0.6}B_{1.2}C_{4.8}$

$LiCa_{0.6}B_{1.2}C_{4.8}$

$Li_{1.2}Ca_{0.6}B_{1.2}C_{4.8}$

Fig. S4

Top and side view of models for as prepared ($Ca_{0.6}B_{1.2}C_{4.8}$) and lithium-intercalated ($Li_xCa_{0.6}B_{1.2}C_{4.8}$) states after structure relaxation by DFT calculations.

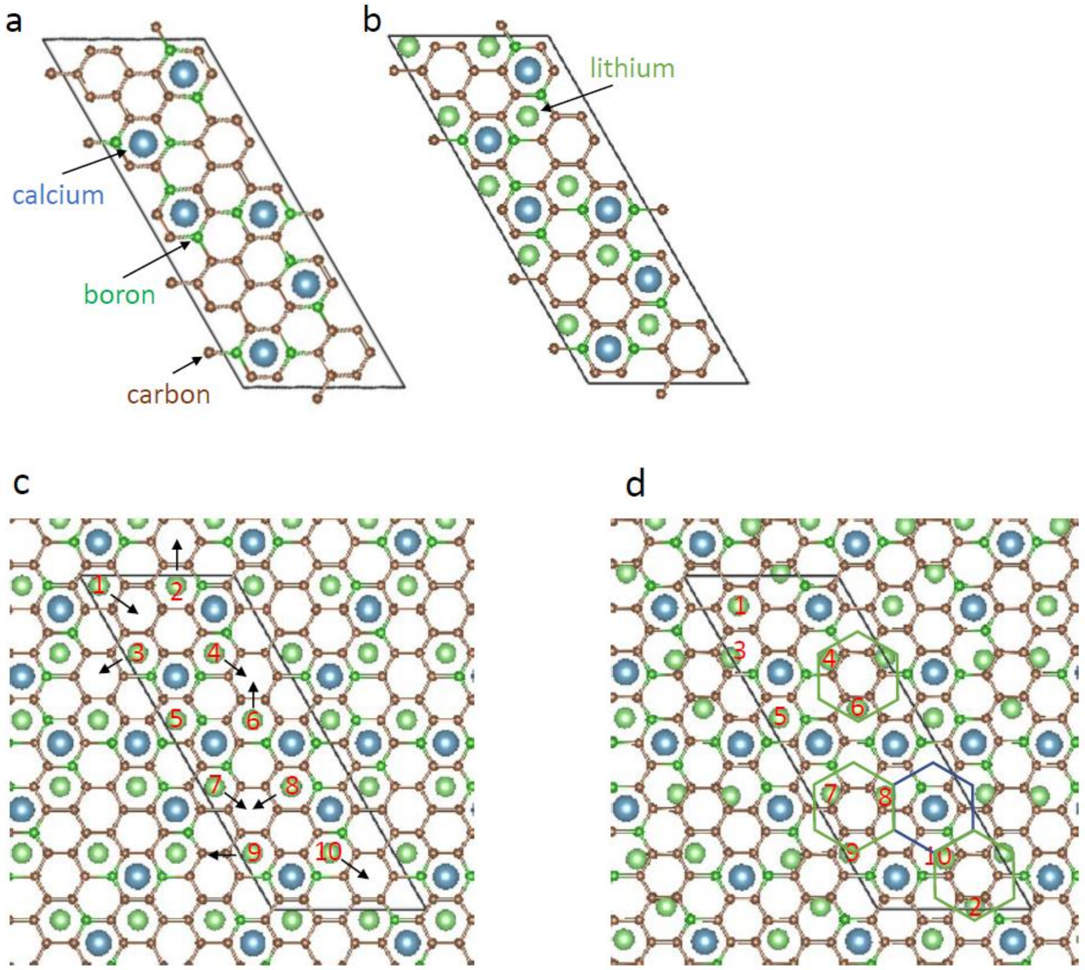

Fig. S5

a) Unit cell of assumed realization of $Ca_{0.6}B_{1.2}C_{4.8}$ b) Unit cell of an initial structure assumed for $LiCa_{0.6}B_{1.2}C_{4.8}$ c) Same as b though the outside of periodic boundaries is also shown. Each Li atom in unit cell is indexed by numbers. Arrows show the direction of Li movement during structure relaxation by the DFT calculation. d) Final configuration after structure relaxation from c). The number for index is consistent with c). Green hexagons indicate the Li dense areas. Blue hexagon indicates an area occupied by a calcium atom.

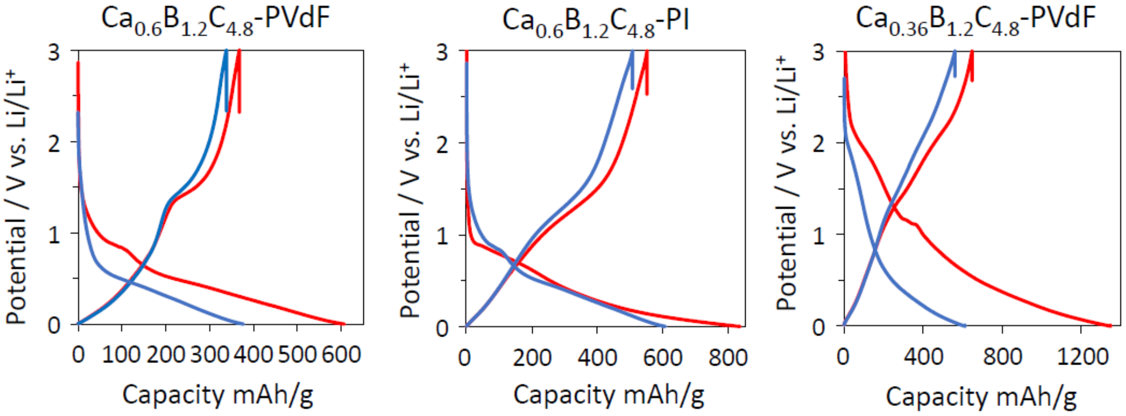

Fig. S6

1st and 2nd cycle curves for $Ca_{0.6}B_{1.2}C_{4.8}$-PVdF, $Ca_{0.6}B_{1.2}C_{4.8}$-PI and $Ca_{0.36}B_{1.2}C_{4.8}$-PVdF

Table S1 Parameters obtained by Rietveld refinement of the synthesized $Ca_{0.6}B_{1.2}C_{4.8}$.

Empirical formula	$Ca_{0.5106(7)}B_{1.2}C_{4.8}$
Crystal system	Hexagonal
Space group	*P6/mmm*, No. 191
Wyckoff position of atoms	Ca: 1a (0,0,0); B, C: 2d (1/3, 2/3, 1/2)
Lattice parameters	a = b = 2.5543(2), c = 4.4359(2) ,$\alpha=\beta=90$, $\gamma=120$
Final R-values	$R_{wp} = 0.06058$, $\chi^2 = 1.237$, $R_p = 0.04680$, $R_B = 0.03541$, $R(F^2) = 0.03095$

Table S2 Concentration of atoms in the synthesized calcium boridecarbides at atomic ratio (mol%).

	Ca	B	C
$Ca_{0.6}B_{1.2}C_{4.8}$	7.74	18.0	74.3
$Ca_{0.75}B_{1.5}C_{4.5}$	10.9	20.9	68.2

Table S3 Ratio of calcium and boron content for as-prepared $Ca_{0.6}B_{1.2}C_{4.8}$ electrode, $Ca_{0.6}B_{1.2}C_{4.8}$ electrode after dipping in electrolyte for 24 hours, and $Ca_{0.36}B_{1.2}C_{4.8}$ prepared by extraction of calcium from $Ca_{0.6}B_{1.2}C_{4.8}$ electrode by applying positive constant current. The value of B is fixed at 1.2.

	Ca	B
$Ca_{0.6}B_{1.2}C_{4.8}$ electrode (as prepared)	0.51	1.2
$Ca_{0.6}B_{1.2}C_{4.8}$ electrode (after dipping in electrolyte)	0.50	1.2
$Ca_{0.36}B_{1.2}C_{4.8}$ (after extracting Ca from $Ca_{0.6}B_{1.2}C_{4.8}$ electrochemically)	0.36	1.2

References

[1] M. Wörle, D. Widmer, F. von Rohr, F. Krumeich, C. Mensing and R. Nesper, *Z. Anorg. Allg. Chem.*, 2010, 636, 1447–1453.

[2] F. Izumi and K. Momma, *Solid State Phenom.*, 2007, 130, 15–20.

[3] R. W. M. Kwok, XPS Peak Fitting Program: XPSPEAK Version 4.1, Department of Chemistry, The Chinese University of Hong Kong.

[4] P. Trucano and R. Chen, *Nature*, 1975, 258, 136–137.

[5] G. Kresse and J. Furthmüller, *Phys. Rev. B*, 1996, 54, 11169−11186.

[6] G. Kresse and J. Furthmüller, *Comput. Mater. Sci.*, 1996, 6, 15−50.

[7] P. E. Blöchl, *Phys. Rev. B*, 1994, 50, 17953−17979.

[8] J. P. Perdew, K. Burke and M. Ernzerhof, *Phys. Rev. Lett.*, 1996, 77, 3865−3868.

[9] S. Grimme, J. Antony, S. Ehrlich and S. Krieg, *J. Chem. Phys.*, 2010, 132, 154104.

[10] S. Grimme, S. Ehrlich and L. Goerigk, *J. Comp. Chem.*, 2011, 32, 1456.

[11] D. Li, P. Dai, Y. Chen, R. Peng, Y. Sun and H. Zhou, *J. Phys. Chem. C*, 2018, 122, 18231−18236.